demonstrate that R80S mutation is a loss-of-function mutation and is responsible for the developmental abnormality and the embryonic death.

Cytological abnormality in ESCO2 *mutant medaka*

Premature centromere separation (PCS) is caused by loss of ESCO2 and is diagnostic of RBS/SC (Schüle *et al.* 2005; Vega *et al.* 2005, 2010; Gordillo *et al.* 2008). To examine whether PCS is observed in R80S mutant medaka, we performed chromosomal analysis of 2-dpf embryos. Mutants showed a significant increase in the chromosomal abnormalities, including aneuploidy, chromosomal hyper-condensation and PCS (Fig. 4A, Table 2). Particularly, chromosomal hyper-condensation and PCS were observed in 39.6% and 6.6% of mutant cells, but only in 4.5% and 0.1% of WT, respectively. Thus, chromosomal abnormalities were observed in mutants similar to that in the *Eco1* mutant of yeast (Skibbens *et al.* 1999), with knocking down of *ESCO2* of HeLa cells (Hou & Zou 2005) and RBS/SC (Vega *et al.* 2005). The chromosomal hyper-condensation may be due to high sensitivity to colchicine in R80S mutants.

We monitored cells in the S-phase (Fig. 4B) and M-phase (Fig. 4C) with BrdU incorporation and an antibody to phosphorylated histone H3, respectively. Morphological differences between WT and mutant embryos were evident in the proliferative zone of the optic tectum, prospective corpus cerebelli, rhombic lips, pectoral fin buds and neural tube. In WT embryos, the proliferative cells were distinguishable and arranged in order. In contrast, the proliferative cells of mutants were widely distributed and out of order. The number of cells in the S- and M-phase tended to be slightly increased in mutants compared to WT embryos.

Next, we attempted cell cycle analysis by flow cytometry (Fig. 4D). In WT embryos, nuclei peaked at 2N DNA (corresponding to cells in the G1-phase), while a small fraction of cells were distributed between 2N and 4N DNA (S-phase), and at 4N DNA (G2/M-phase). Only 9.5% of cells were in the sub-G1 proportion. In contrast, mutant nuclei showed a marked increase in the sub-G1 population (41.2%) at the expense of cells in the G1-phase. Although a clear aneuploidy peak and enrichment of S and G2/M cells were not observed, S and G2/M cells slightly increased in mutants. To confirm the existence of apoptotic cells, we performed a TUNEL assay. In mutant embryos, a large number of cells underwent apoptosis throughout the body, while only a limited number of cells were TUNEL-positive in WT embryos (Fig. 4E). These results suggest that the R80S mutation of ESCO2 induces various chromosomal abnor-

malities including PCS and aneuploidy during cell division, and that the resulting apoptosis may cause developmental delay and eventual embryonic lethality.

Reduction of marker gene expression in ESCO2 *mutant medaka*

Because R80S mutant embryos showed morphological abnormalities, we analyzed the expression patterns of several marker genes, namely, *bf1*, *foxA2*, *iro3*, *krox20*, *notch1a*, *otx1* and *pax6*, as neural development and notochord markers, and *lfng* and *myf5* as somite markers using whole-mount *in situ* hybridization. The gene expression of almost all markers was downregulated and delayed in R80S mutants (Figs 5, S6). The expression of *pax6*, for example, in the eyes, was reduced in mutant embryos compared to WT ones at 2.0 dpf (Fig. 5A). However, when *pax6* expression in 2.0-dpf mutants was compared to 1.0-dpf WT, no significant differences were observed in the zona limitans intrathalamica. Similarly, the gene expression levels of *bf1*, *foxA2*, *iro3* and *lfng* in mutants at 2.0 dpf were similar to those in WT embryos at 1.0 dpf (Fig. S6). The *otx1* and *krox20* expression in 2.0-dpf mutants were similar to 1.5-dpf WT embryos (Fig. S6). Thus, the differences in expression were attributable to developmental retardation in mutants. The expression of *myf5* in mutants resembled 1.0-dpf and 2.0-dpf WT embryos (Fig. 5B). In contrast, strong reduction in *notch1a* expression was observed in mutants at 2.0 dpf (Fig. 5C,D). Because *notch1a* was expressed in WT embryos at 1.0–2.0 dpf, we speculate that this downregulation was not attributable to developmental retardation.

To confirm *notch1a* suppression in mutants, we quantified *notch1a*, *notch1b* (neurogenic markers [Lawson *et al.* 2002], Fig. 6A), and *ascl1a* and *ascl1b* (proneural markers, downstream targets of *notch1a* and *notch1b* in zebrafish [Allende & Weinberg 1994], Fig. 6B) mRNA of 2.0-dpf embryos by quantitative RT–PCR (qRT–PCR). We examined the genotype of all embryos prior to qRT–PCR and classified them into two groups: with and without morphological changes. Forty percent of the homozygous mutants were morphologically normal at 2.0 dpf. The neurogenic marker genes related to *notch* were dramatically suppressed in mutants exhibiting morphological abnormalities (Fig. 6A,B). Namely, the expression of *notch1a*, *notch1b*, *ascl1a* and *ascl1b* in mutants was suppressed by 41%, 50%, 9% and 8%, respectively, compared to the WT embryos. In contrast, no suppression of *notch1b* was observed in the morphologically normal mutants, while all the other neurogenic
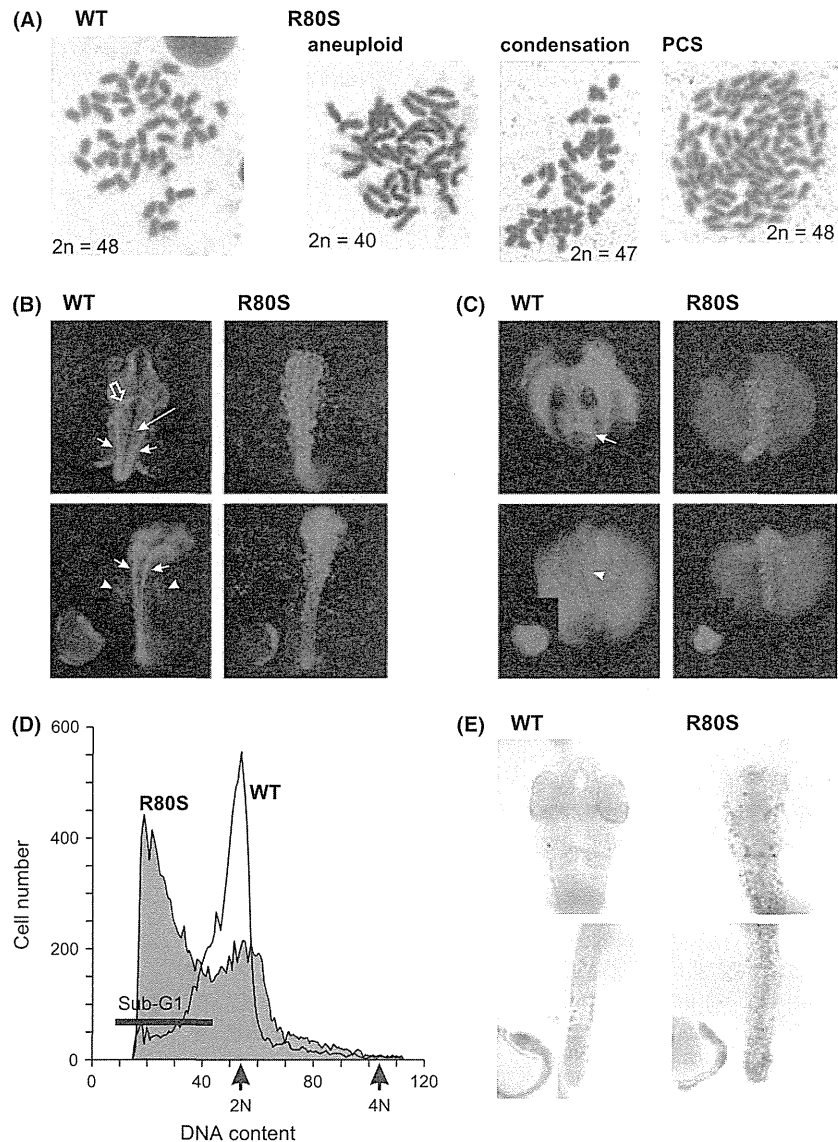
Fig. 4. Cytological abnormality of *ESCO2* mutant medaka. (A) Chromosomal analysis of wild-type (WT, leftmost) and R80S cells. Chromosomal preparation and Giemsa stain were applied to 2.0-days postfertilization (dpf) embryos. In R80S mutants, aneuploidy (shown as 2n = 40 versus 2n = 48 in WT), chromosomal hyper-condensation and premature centromere separation (PCS) were observed. (B) 5-bromodeoxyuridine (BrdU) labeling to detect cells in S-phase at 2.0 dpf. BrdU/Yamamoto solution (0.1%) was injected into the perivitelline space at 2.0 dpf. At 2 h after the injection, the embryos were fixed and immunohistochemically analyzed using anti-BrdU antibody. Top and bottom, dorsal view of the head and pectoral regions, respectively; inset in bottom panels, lateral view. BrdU labeling in the prospective corpus cerebelli (open arrow), rhombic lips (long arrow), the bilateral region of the midline (short arrows) and fin buds (arrowheads) was not detected in R80S mutants. (C) Anti-phosphorylated histone H3-labeling to detect cells in M-phase at 2.0 dpf. The embryos were fixed at 2.0 dpf and immunohistochemically analyzed by anti-phosphorylated histone H3 antibody. Top and bottom, dorsal view of the head and tail, respectively; inset of bottom panels, lateral view. The proliferating zone of the optic tectum and prospective corpus cerebelli (arrow) and the neural tube (arrowhead) was not immunoreactive in R80S mutant. (D) fluorescence-activated cell sorting (FACS) analysis of WT (open) and R80S (shaded) nuclei. The 2.0-dpf embryos were subjected to propidium iodide staining and FACS analysis. Note: the large proportion of R80S nuclei in sub-G1. (E) Terminal deoxynucleotidyl transferase-mediated dUTP nick end labeling assay indicates apoptotic cells throughout the whole body of R80S mutants. Top and bottom, dorsal view of the head and tail, respectively; inset of bottom panels, lateral view.

markers were suppressed by approximately 50% (Fig. 6A,B). We speculate that suppression of *notch1b* expression may be due to gross developmental defects and that the downregulation of *notch1a* is specific to *ESCO2* mutation regardless of developmental delay. Because *ascl1a* and *ascl1b* are downstream of

Table 2. Chromosomal analysis of medaka R80S mutants[†]

Genotype	n	Aneuploidy (%)	Hyper-condensation (%)	PCS (%)	String-like (%)
Embryos[‡]					
ESCO2[WT/WT]	21	42.9	23.8	0.0	0.0
ESCO2[R80S/R80S]	21	76.2*	71.4**	28.6**	19.0*
Cells					
ESCO2[WT/WT]	941	6.2	4.5	0.1	0.1
ESCO2[R80S/R80S]	182	25.3***	39.6***	6.6***	02.7***

*$P < 0.05$; **$P < 0.01$; ***$P < 0.001$, respectively (χ^2-test). [†]R80S embryos (F′2) were derived by crossing R80S (F4) heterozygous mutants of original strain with wild-type fish of another strain K-Kaga. The 2.0-days post fertilization (dpf) embryos were examined. [‡]Embryos with more than 10% of cells exhibiting abnormalities are regarded as abnormal embryos. PCS, premature centromere separation.
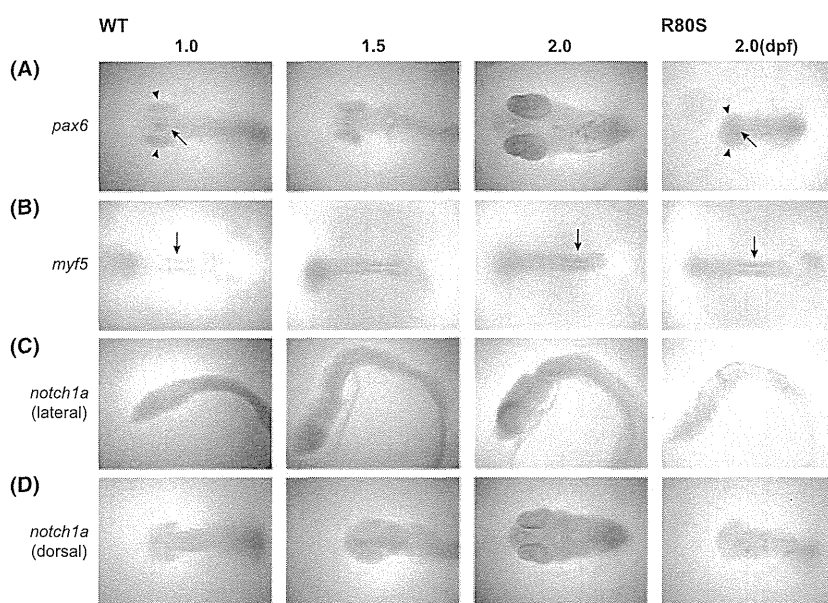

Fig. 5. Expression of marker gene in R80S (rightmost) and wild-type (WT) embryos. (A,B) Dorsal view of the *pax6* (A) and *myf5* (B) expression in the head and tail region, respectively. Expression of *pax6* in optic vesicles (arrowheads) is unclear in R80S mutant, but the expression in the zona limitans intrathalamica (arrows) is evident in both WT and R80S mutants. Expression of *myf5* (arrows) in R80S embryo resembles 1.0- and 2.0-day postfertilization (dpf) WT embryos. Lateral (C) and dorsal (D) view of the *notch1a* expression. Note: *notch1a* expression disappears in R80S mutant.

both *notch1a* and *notch1b*, the reduction of *ascl1a* and *ascl1b* may be more pronounced in morphologically abnormal mutants.

Next, we examined *GATA-1* and *notch3* (vascular differentiation markers in zebrafish [Lawson *et al.* 2001, 2002], Fig. 6C) because the heart was malformed in mutants. They were suppressed by 57% and 30%, respectively, in mutants with morphological abnormalities. In mutants with normal morphology, no significant reduction in *GATA-1* was observed (Fig. 6C), suggesting that *GATA-1* suppression may accompany general developmental delay, as is the case with *notch1b*. To confirm these data, we investigated the gene expression in morphants. We used the ATG mo and 5mis mo (as control), because ATG mo inhibits maternal and embryonic *ESCO2*. The ATG mo

morphants showed suppression of *notch1a* (by 67%), *notch1b* (66%) and *notch3* (71%) (Fig. 6D,E). Downregulation of *notch1b* may be attributable to the developmental delay in ATG mo morphants (Fig. 3A). Thus, *ESCO2* mutation causes downregulation of *notch1a* and *notch3*. In summary, these data suggest that *ESCO2* may play a role in embryogenesis through upregulation of critical genes such as *notch1a* and *notch3*.

Discussion

Establishment of RBS/SC model medaka

We established a medaka model of RBS/SC using the TILLING method and characterized it using a reverse
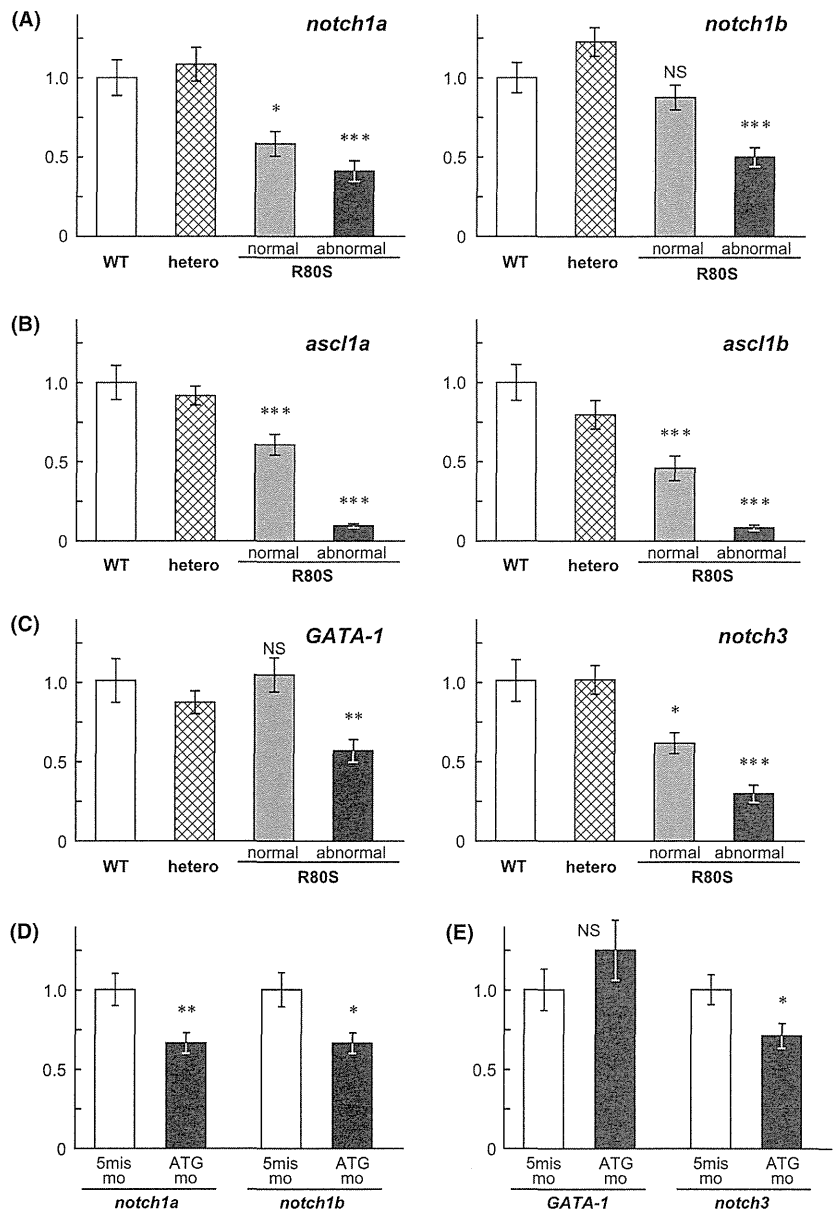
Fig. 6. Suppression of the expression of several genes in R80S embryos (A–C) and *ESCO2*-knockdown morphants (D,E). The expression of neurogenesis markers, *notch1a* and *notch1b* (A), neural progenitor markers, *ascl1a* and *ascl1b* (B) and vascular differentiation markers, *GATA-1* and *notch3* (C) in wild-type (WT), heterozygous (*ESCO2^{R80S/WT}*, hetero) and homozygous (*ESCO2^{R80S/R80S}*, R80S) mutants (2.0 days postfertilization [dpf]) was investigated by quantitative reverse transcription polymerase chain reaction. Normal and abnormal indicate apparently normal mutants and developmentally abnormal mutants, respectively. The expression of *notch1a* and *notch1b* (D) and *GATA-1* and *notch3* (E) in morphants (2.0 dpf) with the injection of 5mis mo (control) or ATG mo was examined. NS, *, ** and *** indicate $P \geq 0.05$, $P < 0.05$, $P < 0.01$ and $P < 0.001$, respectively, compared to WT or control embryos; ANOVA and Tukey's test, $n = 13$–14 (A–C); Student's t-test, $n = 13$ (D,E).

genetic approach. Morpholino antisense oligonucleotide is a very useful tool when using medaka or zebrafish as an animal model to efficiently reduce the expression of a gene of interest. However, it is sometimes difficult to ascertain the cause–effect relationship because morpholinos are often complicated by off-target effect. It should be especially difficult to analyze the morphants when the phenotypes vary as in RBS/SC. The mutant has a great advantage over morphants in that the gene alteration is fixed in the genome and the phenotypes can be analyzed in the uniform genetic background. Compared to other classical gene disruption methods such as homologous recombination and transposon/retrovirus insertion,

TILLING has the great advantage of missense mutant recovery. Amino acid (a.a.) substitutions reveal the unexpected role of a protein, which cannot be obtained by knockout (KO) and knockdown methods. Missense mutants are particularly useful in the analysis of essential genes because simple disruption of the gene would cause lethality at the cellular or animal level. To our knowledge, *ESCO2*-KO mice have not been reported to date. Fish such as medaka are suited to investigation of the gene function during embryonic development as they develop *ex vivo*. The development of organs in fish share common molecular pathways with mammals. The developmental abnormality and death during development can be closely monitored in fish while

many of the lethal phenotypes may be overlooked in humans. Taken together, our system by using medaka could provide a powerful tool for investigating unidentified missense mutations in autosomal recessive disorders *in vivo*, even in embryonic lethal mutants.

The R80S mutant was created by ethyl nitroso urea (ENU) mutagenesis, which randomly introduces point mutations throughout the genome. In order to examine whether the observed phenotype was related to the R80S mutation, and to exclude the possibility that it was not derived from other mutation(s), we took two approaches: *in vivo* morpholino injections into the fertilized medaka eggs and linebreeding. The *ESCO2* morphants exhibited developmental abnormality and reduction of *notch1a* and *notch3* expression similar to that observed in the mutants. Moreover, the developmental and cytological abnormalities observed in mutants with a K-Cab (southern population) genetic background could be transferred to K-Kaga (northern population) genetic background by crossing original mutants with WT K-Kaga. Therefore, we suggest that the R80S mutation is responsible for the observed phenotypes.

Clinical feature in RBS/SC model medaka

The variety of phenotypes among individuals and the lack of a clear correlation between genotype and phenotype are some of the clinical features of RBS/SC. It has been shown that the same mutation results in different phenotypes in RBS/SC (Schüle *et al.* 2005;

Vega *et al.* 2005, 2010; Gordillo *et al.* 2008). Recently, Mönnich *et al.* (2011) demonstrated that *ESCO2*-KD zebrafish showed craniofacial and fin abnormality. We summarized the phenotype of RBS/SC, R80S mutants, medaka *ESCO2* morphants (present study) and zebrafish *ESCO2* morphants (Mönnich *et al.* 2011) (Table 3). We also observed phenotypic diversity in our mutant medaka: craniofacial abnormalities, cardiac defect, growth retardation and PCS. RBS/SC is characterized by craniofacial abnormalities including bilateral cleft lip and/or palate, micrognathia, hypertelorism, exophthalmos, downslanting palpebral fissures, malar hypoplasia, hypoplastic nasal alae and ear malformation (Gordillo *et al.* 2006). R80S mutants exhibited a severe phenotype in the head region and were deficient in all head elements except for the eyes, even which showed developmental delay and incorrect structure. Thus, the morphological phenotype of the R80S mutant was very similar to RBS/SC and zebrafish *ESCO2* morphants except for limb abnormalities. The upper and lower limbs of humans and the pectoral and pelvic fins of medaka are evolutionarily derived from the same origins (Hinchliffe 2002). However, long bone growth in the stylopod and zeugopod is absent in the fins. Moreover, the fins have no part that is homologous to the autopod, which constitutes the distal part of mammalian limbs (Hinchliffe 2002). Therefore, phocomelia, long bone hypoplasia, ectrodactylia and brachydactylia cannot be detected in fish. In zebrafish *ESCO2* morphants, shorter and smaller fins were observed (Mönnich *et al.* 2011). Our R80S

Table 3. Summary of phenotypes of Roberts syndrome/SC phocomelia (RBS/SC) and medaka and zebrafish models

RBS/SC (human)	R80S mutants (medaka)	Morphants (medaka)	Morphants[†] (zebrafish)
Autosomal recessive	Autosomal recessive		
Intra uterine fetal death	Embryonic lethal	Survive	Embryonic lethal
Pre- and postnatal growth retardation	Developmental delay	Developmental delay	
	Small size	Small size	Small size
	Body axis abnormality	Body axis abnormality	Body axis abnormality
Craniofacial abnormality			
Microcephaly	Microcephaly	Normal	Smaller heads
Hyper telorism	Smaller and abnormal eye	Normal	Smaller eye
Hypoplastic nasal alae	Lack of nasal part	Normal	ND
Malar hypoplasia	Cartilage defect	ND	ND
Cleft lip and palate	Lack of mouth part	Normal	Lack of jaw
Limb abnormality			
Phocomelia	ND	ND	ND
Ulnar defects	ND	ND	ND
Radial defects	ND	ND	ND
Thumb defects	Normal (delayed)	Normal	Shorter and smaller fin
Renal abnormality	ND	ND	ND
Heart defect	Heart malformation	Heart malformation	Cardiac edema
Mental retardation	ND	ND	ND
Premature centromere separation	Premature centomere separation	ND	ND

[†]After Mönnich *et al.* 2011. ND, not determined.

mutants had normal pectoral fins. However, some of them exhibited developmental delay. Therefore, shorter and smaller fins of zebrafish morphants may correspond to the mutant fins developmentally delay. Medaka *ESCO2* morphants also had normal pectoral fins. The effect of morpholino was weaker in medaka than in zebrafish. This may be due to the time frame of morpholino action as medaka develops much more slowly than zebrafish and the effect of morpholino may be reduced by the time these organs are formed.

R80S mutants also exhibited developmental arrest by 2 dpf with incomplete penetrance (Table 1). Most of the escapers exhibited heart malformation and/or body axis abnormalities. This may be pertinent to the phenotypic variation observed in humans. Concerning congenital cardiac abnormality, atrial septal defect, ventricular septal defect and patent ducts arteriosus were reported (Gordillo *et al.* 2006). The escapers of R80S mutant and some of *ESCO2* morphants showed looping defect. Disturbance in cardiac looping is thought to cause congenital cardiac malformations (Männer 2009).

ESCO2-KD zebrafish showed cell cycle arrest and apoptosis with caspase activation (Mönnich *et al.* 2011). In R80S mutant of medaka, we could not clearly detect significant cell cycle arrest. This disagreement may be attributable to the difference of species or to the difference of knockdown (zebrafish) and missense mutant (medaka). We also detected apoptosis throughout the body in R80S mutants. This apoptosis may be associated with caspase activation, as in zebrafish. Moreover, microarray analysis revealed the gene regulated by ESCO2 in zebrafish and some gene regulation overlaps with cohesin-dependent transcription (Rhodes *et al.* 2010; Mönnich *et al.* 2011).

R80S mutation is responsible for embryonic death, and deficiency of Eco1 in yeast causes cellular lethality. On the contrary, RBS/SC patients can give birth. It was reported that the related molecule, ESCO1 in humans, and suggested that ESCO1 and ESCO2, play distinct roles in cell cycle progression (Hou & Zou 2005). Although ESCO1 and ESCO2 acetylate SMC3, the knocking down of *ESCO1* is more effective on the SMC acetylation than that of *ESCO2* in humans (Zhang *et al.* 2008). The different effect of functional deficiency in ESCO2 between RBS/SC patients and R80S mutants may be explainable by the difference of functionalization of ESCO1 and ESCO2. The function of ESCO1 in medaka needs to be elucidated. On the other hand, the mutant medaka showed more severe phenotypes than RBS/SC and morphants of medaka and zebrafish. Only mutant medaka is embryonically lethal. RBS/SC patients are rare and RBS/SC is characterized by intrauterine fetal death. A few R80S

mutants can live up to adult fish. Thus, RBS/SC patients may be escapers as in R80S mutants. The escapers of R80S mutants will be analyzed in a future study.

R80S mutation

We have found that the mutation in the conserved amino acid (a.a.) in the N-terminal portion of ESCO2, R80 (in human K), disrupts the establishment of cohesion function of ESCO2, demonstrating the importance of this previously undescribed region of this protein. This is the first case in which a missense mutation outside the acetyltransferase domain causes the loss-of-function phenotype. The region (73–84 a.a.) including R80 is well conserved from fish to humans, although the mutation in this region has not been reported in RBS/SC. ECO1 lacks this region. Although Eso1 (Tanaka *et al.* 2010), budding yeast homologue, deco (Williams *et al.* 2003), *Drosophila* homologue and ESCO1 (Hou & Zou 2005) of humans contain extradomain at the N-termius, no motif or similarity have been found in the N-terminal portion of ESCO2. The molecular function of this conserved region is of special interest.

Variety of clinical features in RBS/SC

The *ESCO2* expression in the proliferating region and the chromosomal phenotype, namely, PCS, caused by the R80S mutation indicate that ESCO2 plays an important role in cell division in medaka. In other species, ESCO2 functions in the establishment of sister chromatid cohesion via acetylation of the cohesin complex (Rolef Ben-Shahar *et al.* 2008; Unal *et al.* 2008; Zhang *et al.* 2008). Therefore, the R80S mutation of ESCO2 may cause a reduction of cohesin complex acetylation, resulting in an anti-establishment state in sister chromatid cohesion during S-phase similar to that in other species including humans. On the other hand, RBC/SC has a variety of clinical features (Schüle *et al.* 2005; Vega *et al.* 2005, 2010; Gordillo *et al.* 2008). The same mutation of ESCO2 causes different phenotypes. R80S mutants also have a variety of clinical phenotypes. Pathological features in the establishment of sister chromatid cohesion are attributable to a lack of ESCO2 function in cell division. However, this is not sufficient to explain the variety in the clinical features. The cohesin complex, the target of ESCO2, causes Cornelia de Lange syndrome (CdLS) (OMIM 122470, 300590 and 610759). CdLS also has a variety of clinical features (Dorsett 2007; Liu & Krantz 2009). The clinical features of CdLS are distinct from RBS/SC, but with some overlap (Liu & Krantz 2009). Recently, cohesion-mediated gene regulation was

demonstrated in *Drosophila*, zebrafish, mice and humans. Homeobox gene expression is required for Nipped-B, a cohesin regulator in *Drosophila* (Dorsett 2009). The gene expressions of *runx1* and *runx3* (transcription factors) are required for Rad21 and Smc3 (components of the cohesin complex) in zebrafish (Horsfield *et al.* 2007). Genome-wide chromatin immunoprecipitation experiments in human and mouse cells have revealed co-localization of cohesin and CTCF, a zinc-finger protein with enhancer blocking and barrier activities (Parelho *et al.* 2008; Stedman *et al.* 2008; Wendt *et al.* 2008). CTCF is thought to have a potential function in directly regulating gene transcription both positively and negatively (Ishihara *et al.* 2006; Chernukhin *et al.* 2007). ESCO2 functions in establishment of sister chromatid cohesion by acetylation of the cohesin complex. Therefore, mutation of ESCO2 may cause lack of functional cohesin. Consequently, it is suggested that mutation of ESCO2 affects the expression of several genes. In this study, we demonstrated that R80S mutation actually suppresses *notch1a*, its downstream genes and *notch3* expression. Downregulation of *notch1a* and its downstream gene expression result from the mutation of the cohesin component in zebrafish (Horsfield *et al.* 2007). Therefore, we propose that the neural and heart malformations may involve downregulation of these genes in R80S mutant medaka and RBS/SC. The clinical feature of cardiac defects in R80S mutants is similar to the medaka knocking-down of congenital heart disease 5 (*mCHD5*) gene function (Murata *et al.* 2009). *Notch3* suppressed in ESCO2 R80S mutant may be involved in *mCHD5* expression. Recently, cohesin-independent regulation of gene expression by Eco1 was reported (Choi *et al.* 2010). Eco1 suppresses transcription via association with histone demethylase, LSD1, to convert chromatin to an inactive state. Thus, ESCO2 regulates the expression of several genes. Research on the genes regulated by ESCO2 is an interesting area for further study. The functional analyses of ESCO2 have only been performed at cellular level so far. This mutant medaka enables analysis at a whole-body level, particularly, in the early embryonic development. The mechanisms producing the pathological variety of RBS/SC will be elucidated.

In conclusion, we isolated *ESCO2* mutant medaka from the TILLING library and characterized it using a reverse genetic approach. The *ESCO2^{R80S/R80S}* homozygous mutants had phenotypic features reminiscent of RBS/SC. From the gene expression analysis, some gene expression was downregulated in mutants. Thus *ESCO2* mutant medaka is the animal model for RBS/SC and a valuable resource for future research.

References

Aizawa, K., Shimada, A., Naruse, K., Mitani, H. & Shima, A. 2003. The medaka midblastula transition as revealed by the expression of the paternal genome. *Gene Expr. Patterns* **3**, 43–47.

Allende, M. L. & Weinberg, E. S. 1994. The expression pattern of two zebrafish achaete-scute homolog (ash) genes is alterd in the embryonic brain of the cyclops mutant. *Dev. Biol.* **166**, 509–530.

Candal, E., Alunni, A., Thermes, V., Jamen, F., Joly, J.-S. & Bourrat, F. 2007. *Ol-insm1b*, a SNAG family transcription factor involved in cell cycle arrest during medaka development. *Dev. Biol.* **309**, 1–17.

Chernukhin, I., Shamsuddin, S., Kang, S. Y., Bergström, R., Kwon, Y.-W., Yu, W. Q., Whitehead, J., Mukhopadhyay, R., Docquier, F., Farrar, D., Morrison, I., Vigneron, M., Wu, S. Y., Chiang, C. M., Loukinov, D., Lobanenkov, V., Ohlsson, R. & Klenova, E. 2007. CTCF interacts with and recruits the largest subunit of RNA polymerase II to CTCF target sites genome-wide. *Mol. Cell. Biol.* **27**, 1631–1648.

Choi, H. K., Kim, B.-J., Seo, J.-H., Kang, J.-S., Cho, H. & Kim, S.-T. 2010. Cohesion establishment factor, Eco1 represses transcription via association with histone demethylase, LSD1. *Biochem. Biophys. Res. Commun.* **394**, 1063–1068.

Dorsett, D. 2007. Roles of the sister chromatid cohesion apparatus in gene expression, development, and human syndromes. *Chromosoma* **116**, 1–13.

Dorsett, D. 2009. Cohesin, gene expression and development: lessons from *Drosophila*. *Chromosome Res.* **17**, 185–200.

Furutani-Seiki, M., Sasado, T., Morinaga, C., Suwa, H., Niwa, K., Yoda, H., Deguchi, T., Hirose, Y., Yasuoka, A., Henrich, T., Watanabe, T., Iwanami, N., Kitagawa, D., Saito, K., Asaka, S., Osakada, M., Kunimatsu, S., Momoi, A., Elmasri, H., Winkler, C., Ramialison, M., Loosli, F., Quiring, R., Carl, M., Grabher, C., Winkler, S., Del Bene, F., Shinomiya, A., Kota, Y., Yamanaka, T., Okamoto, Y., Takahashi, K., Todo, T., Abe, K., Takahama, Y., Tanaka, M., Mitani, H., Katada, T., Nishina, H., Nakajima, N., Wittbrodt, J. & Kondoh, H. 2004.

A systematic genome-wide screen for mutations affecting organogenesis in Medaka *Oryzias latipes*. *Mech. Dev.* **121**, 647–658.

Gordillo, M., Vega, H., Trainer, A. H., Hou, F., Sakai, N., Luque, R., Kayserili, H., Basaran, S., Skovby, F., Hennekam, R. C. M., Uzielli, M. L., Schnur, R. E., Manouvrier, S., Chang, S., Blair, E., Hurst, J. A., Forzano, F., Meins, M., Simola, K. O., Raas-Rothschild, A., Schultz, R. A., McDaniel, L. D., Ozono, K., Inui, K., Zou, H. & Jabs, E. W. 2008. The molecular mechanism underlying Roberts syndrome involves loss of ESCO2 acetyltransferase activity. *Hum. Mol. Genet.* **17**, 2172–2180.

Gordillo, M., Vega, H. & Jabs, E. W. 2006. Roberts syndrome. In: *GeneReviews* (eds Pagon RA, Bird TD, Dolan CR, Stephens K & Adam MP). University of Washington, Seattle, WA. 1993.

Hinchliffe, J. R. 2002. Develomental basis of limb evolution. *Int. J. Dev. Biol.* **46**, 835–845.

Horsfield, J. A., Anagnostou, S. H., Hu, J. K.-H., Cho, K. H. Y., Geisler, R., Kieschke, G., Crosier, K. E. & Crosier, P. S. 2007. Cohesin-dependent regulation of *Runx* genes. *Development* **134**, 2639–2649.

Hou, F. & Zou, H. 2005. Two human orthologues of Eco1/Ctf7 acetyltransferases are both required for proper sister-chromatid cohesion. *Mol. Biol. Cell* **16**, 3908–3918.

Iijima, N. & Yokoyama, T. 2007. Apoptosis in the medaka embryo in the early developmental stage. *Acta Histochem. Cytochem.* **40**, 1–7.

Ishihara, K., Oshimura, M. & Nakao, M. 2006. CTCF-dependent chromatin insulator is linked to epigenetic remodeling. *Mol. Cell* **23**, 733–742.

Ishikawa, Y. 2000. Medakafish as a model system for vertebrate developmental genetics. *BioEssays* **22**, 487–495.

Ivanov, D., Schleiffer, A., Eisenhaber, F., Mechtler, K., Haering, C. H. & Nasmyth, K. 2001. Eco1 is a novel acetyltransferase that can acetylate proteins involved in cohesion. *Curr. Biol.* **12**, 323–328.

Iwamatsu, T. 1994. Stages of normal development in the medaka *Oryzias latipes*. *Zool. Sci.* **11**, 825–839.

Kage, T., Takeda, H., Yasuda, T., Maruyama, K., Yamamoto, N., Yohimoto, M., Araki, K., Inohaya, K., Okamoto, H., Yasumasu, S., Watanabe, K., Ito, H. & Ishikawa, Y. 2004. Morphogenesis and regionalization of the medaka embryonic brain. *J. Comp. Neurol.* **476**, 219–239.

Kasahara, M., Naruse, K., Sasaki, S., Nakatani, Y., Qu, W., Ahsan, B., Yamada, T., Nagayasu, Y., Doi, K., Kasai, Y., Jindo, T., Kobayashi, D., Shimada, A., Toyoda, A., Kuroki, Y., Fujiyama, A., Sasaki, T., Shimizu, A., Asakawa, S., Shimizu, N., Hashimoto, S., Yang, J., Lee, Y., Matsushima, K., Sugano, S., Sakaizumi, M., Narita, T., Ohishi, K., Haga, S., Ohta, F., Nomoto, H., Nogata, K., Morishita, T., Endo, T., Shin-I, T., Takeda, H., Morishita, S. & Kohara, Y. 2007. The medaka draft genome and insights into vertebrate genome evolution. *Nature* **447**, 714–719.

Lawson, N. D., Scheer, N., Pham, V. N., Kim, C.-H., Chitins, A. B., Campos-Ortega, J. & Westein, B. M. 2001. Notch signaling is required for arterial-venous differentitation during embryonic vascular development. *Development* **128**, 3675–3683.

Lawson, N. D., Vogel, A. M. & Weinstein, B. M. 2002. *Sonic hedgehog* and *vascular endothelial growth factor* act upstream of the notch pathway during arterial endothelial differentiation. *Dev. Cell* **3**, 127–136.

Liu, J. & Krantz, I. D. 2009. Cornelia de Lange syndrome, cohesin, and beyond. *Clin. Genet.* **76**, 303–314.

Männer, J. 2009. The anatomy of cardiac looping: a step towards the understanding of the morphogenesis of several forms of congenital cardiac malformations. *Clin. Anat.* **22**, 21–35.

Moldovan, G. L., Pfander, B. & Jentsch, S. 2006. PCNA controls establishment of sister chromatid cohesion during S phase. *Mol. Cell* **23**, 723–732.

Mönnich, M., Kuriger, Z., Print, C. G. & Horsfield, J. A. 2011. A zebrafish model of Roberts syndrome reveals that esco2 depletion interferes with development by disrupting the cell cycle. *PLoS ONE* **6**, e20051.

Murata, K., Degmetich, S., Kinoshita, M. & Shimada, E. 2009. Expression of the congenital heart disease 5/tryptophan rich basic protein homologue gene during heart development in medaka fish, *Oryzias latipes*. *Dev. Growth Differ.* **51**, 95–107.

Nguyen, V., Deschet, K., Henrich, T., Godet, E., Joly, J.-S., Wittbridt, J., Chourrout, D. & Bourrat, F. 1999. Morphogenesis of the optic tectum in the medaka (*Oryzias latipes*): a morphological and molecular study with special emphasis on cell proliferation. *J. Comp. Neurol.* **413**, 385–404.

Nishihara, M., Yamada, M., Nozaki, M., Nakahira, K. & Yanagihara, I. 2010. Transcriptional regulation of the human establishment of cohesion 1 homolog 2 gene. *Biochem. Biophys. Res. Commun.* **393**, 111–117.

Onn, I., Guacci, V. & Koshland, D. E. 2009. The zinc finger of Eco1 enhances its acetyltransferase activity during sister chromatid cohesion. *Nucleic Acids Res.* **37**, 6126–6134.

Parelho, V., Hadjur, S., Spivakov, M., Leleu, M., Sauer, S., Gregson, H. C., Jarmuz, A., Canzonetta, C., Webster, Z., Nesterova, T., Cobb, B. S., Yokomori, K., Dillon, N., Aragon, L., Fisher, A. G. & Merkenschlager, M. 2008. Cohesins functionally associate with CTCF on mammalian chromosome arms. *Cell* **132**, 422–433.

Rembold, M., Lahiri, K., Foulkes, N. S. & Wittbrodt, J. 2006. Transgenesis in fish: efficient selection of transgenic fish by co-injection with a fluorescent reporter construct. *Nat. Protoc.* **1**, 1133–1139.

Rhodes, J. M., Bentley, F. K., Print, C. G., Dorsett, D., Misulovin, Z., Dickinson, E. J., Crosier, K. E., Crosier, P. S. & Horsfield, J. A. 2010. Positive regulation of c-*Myc* by cohesin is direct, and evolutionarily conserved. *Dev. Biol.* **344**, 637–649.

Rolef Ben-Shahar, T., Heeger, S., Lehane, C., East, P., Flynn, H., Skehel, M. & Uhlmann, F. 2008. Eco1-dependent cohesin acetylation during establishment of sister chromatid cohesion. *Science* **321**, 563–566.

Schüle, B., Oviedo, A., Johnston, K., Pai, S. & Francke, U. 2005. Inactivating mutations in ESCO2 cause SC phocomelia and Roberts syndrome: no phenotype-genotype correlation. *Am. J. Hum. Genet.* **77**, 1117–1128.

Skibbens, R. V., Corson, L. B., Koshland, D. & Hieter, P. 1999. Ctf7p is essential for sister chromatid cohesion and links mitotic chromosome structure to the DNA replication machinery. *Genes Dev.* **13**, 307–319.

Stedman, W., Kang, H., Lin, S., Kissil, J. L., Bartolomei, M. S. & Lieberman, P. M. 2008. Cohesins localize with CTCF at the KSHV latency control region and at cellular c-myc and H19/Igf2 insulators. *EMBO J.* **27**, 654–666.

Tanaka, K., Yonekawa, T., Kawasaki, Y., Kai, M., Furuya, K., Iwasaki, M., Murakami, H., Yanagida, M. & Okayama, H. 2010. Fission yeast Eso1p is required for establishing sister chromatid cohesion during S phase. *Mol. Cell. Biol.* **20**, 3459–3469.

Taniguchi, Y., Takeda, S., Furutani-Seiki, M., Kamei, Y., Todo, T., Sasado, T., Deguchi, T., Kondoh, H., Mudde, J.,

Yamazoe, M., Hidaka, M., Mitani, H., Toyaoda, A., Sakaki, Y., Plasterk, R. H. & Cuppen, E. 2006. Generation of medaka gene knockout models by target-selected mutagenesis. *Genome Biol.* **7**, R116.

Terasaki, H., Murakami, R., Yasuhiko, Y., Shin-i, T., Kohara, Y., Saga, Y. & Takeda, H. 2006. Transgenic analysis of the medaka *mesp-b* enhancer in somitogenesis. *Dev. Growth Differ.* **48**, 153–168.

Terret, M. E., Sherwood, R., Rahman, S., Qin, J. & Jallepalli, P. V. 2009. Cohesin acetylation speeds the replication fork. *Nature* **462**, 231–234.

Unal, E., Heidinger-Pauli, J. M., Kim, W., Guacci, V., Onn, I., Gygi, S. P. & Koshland, D. E. 2008. A molecular determinant for the establishment of sister chromatid cohesion. *Science* **321**, 566–569.

Vega, H., Trainer, A. H., Gordillo, M., Crosier, M., Kayserili, H., Skovby, F., Giovannucci Uzielli, M. L., Schnur, R. E., Manouvrier, S., Blair, E., Hurst, J. A., Forzano, F., Meins, M., Simola, K. O. J., Raas-Rothschild, A., Hennekam, R. C. M. & Jabs, E. W. 2010. Phenotypic variability in 49 cases of ESCO2 mutations, including novel missense and codon deletion in the acetyltransferase domain, correlates with ESCO2 expression and established the clinical criteria for Roberts syndrome. *J. Med. Genet.* **47**, 30–37.

Vega, H., Waisfisz, Q., Gordillo, M., Sakai, N., Yanagihara, I., Yamada, M., van Gosliga, D., Kayserili, H., Xu, C., Ozono, K., Jabs, E. W., Inui, K. & Joenje, H. 2005. Roberts syndrome is caused by mutations in ESCO2, a human homolog of yeast ECO1 that is essential for the establishment of sister chromatid cohesion. *Nat. Genet.* **37**, 468–470.

Wendt, K. S., Yoshida, K., Itoh, T., Bando, M., Koch, B., Schirghuber, E., Tsutsumi, S., Nagae, G., Ishihara, K., Mishiro, T., Yahata, K., Imamoto, F., Aburatani, H., Nakao, M., Imamoto, N., Maeshima, K., Shirahige, K. & Peters, J. M. 2008. Cohesin mediates transcriptional insulation by CCCTC-binding factor. *Nature* **451**, 796–801.

Westerfield, M. 2000. *The Zebrafish Book. A Guide for the Laboratory Use of Zebrafish (Danio rerio)*, 4th edn. University of Oregon Press, Eugene, Oregon.

Whitfield, M. L., Sherlock, G., Saldanha, A. J., Murray, J. I., Ball, C. A., Alexander, K. E., Matese, J. C., Perou, C. M., Hurt, M. M., Brown, P. O. & Botstein, D. 2000. Identification of genes periodically expressed in the human cell cycle and their expression in tumors. *Mol. Biol. Cell* **13**, 1977–2000.

Williams, B. C., Garrett-Engele, C. M., Li, Z., Williams, E. V., Rosenman, E. D. & Goldberg, M. L. 2003. Two putative acetyltransferases, san and deco, are required for establishing sister chromatid cohesion in *Drosophila*. *Curr. Biol.* **13**, 2025–2036.

Yasutake, J., Ihohaya, K. & Kudo, A. 2004. *Twist* functions in vertebral column formation in medaka, *Oryzias latipes*. *Mech. Dev.* **121**, 883–894.

Zar, J. H. 2010. *Biostatistical Analysis*, 5th edn. Pearson Education Inc., Upper Saddle River, NJ.

Zhang, J., Shi, X., Li, Y., Kim, B.-J., Jia, J., Huang, Z., Yang, T., Fu, X., Jung, S. Y. & Wang, Y. 2008. Acetylation of Smc3 by Eco1 is required for S phase sister chromatid cohesion in both human and yeast. *Mol. Cell* **31**, 143–151.

Supporting Information

Additional Supporting Information may be found in the online version of this article:

Figure S1. Alignment of deduced amino acid sequences of ESCO2 in medaka (*Oryzias latipes*), human (*Homo sapiens*, accession no. NP_001017420), mouse (*Mus musculus*, accession no. NP_082315) and zebrafish (*Danio rerio*, accession no. Q5SPR8).

Figure S2. Expression of *ESCO2* in early development of medaka embryo.

Figure S3. Developmental profile of the expression alleles of *ESCO2*.

Figure S4. Construction of morpholinos.

Figure S5. Pectoral width of WT (empty bars) and R80S (solid bars) embryos (2.0 dpf, A), and morphants (2.0 dpf) with 300 nmol/L of 5mis mo (empty bars), ATG mo (solid bars) or E2I2 mo (shaded bars) injected just after fertilization (B). dpf, days postfertilization; WT, wild type.

Figure S6. Expression of marker gene in R80S (uppermost) and wild-type embryos.

Table S1. Primer using for cloning, genotyping and real-time polymerase chain reaction.

Please note: Wiley-Blackwell are not responsible for the content or functionality of any supporting materials supplied by the authors. Any queries (other than missing material) should be directed to the corresponding author for the article.